Noname manuscript No.
(will be inserted by the editor)

Rotational self-friction problem of elastic rods

Mohamed Ali Latrach · Mourad Chamekh

Received: date / Accepted: date

Abstract The aim of this paper is to extend the modeling of a hyperelastic rod undergoing large displacements with tangential self-friction to their modeling with rotational self-friction. As well as the discontinuity of contact force into a contact region not known in advance, taking into account the effects of friction in this problem type underlies more serious modeling, mathematical and numerical analysis difficulties. In this paper, we present an accurate modeling of rotational and tangential self-friction with Coulomb's law and also describe an augmented Lagrangian method to present a weak variational formulation approach of this problem. We then use the minimization method of the total energy to present an existence result of solution for the nonlinear penalized formulation. Finally, we give the linearization and the finite-element discretization of the weak variational formulation that can be useful for a numerical implementation.

Keywords Cosserat rods · Contact distance · Self-friction · Augmented Lagrangian method · Finite elements

Mathematics Subject Classification (2020) MSC code1 · MSC code2 · more

Mohamed Ali Latrach
University of Tunis El Manar National Engineering School at Tunis LAMSIN, B.P. 37, 1002 Tunis-Belvédère Tunisia
Tel.: +216 22 054 266
E-mail: mohamedali.latrach@enit.utm.tn

Mourad Chamekh
Mathematics Department College of Science and Arts AlKamel University of Jeddah Saudi Arabia
E-mail: chamekhmourad1@gmail.com

1 Introduction

Modeling beam to beam contact, beam to surface contact or self-contact in an elastic rod with or without friction has practical applications in many fields of industrial engineering and biomechanics, such as: the pipelines-soil interaction and drill-string dynamics in oil industries [11, 27], beams-slab interaction in civil engineering and subsea cables installation in marine industries [16, 24, 28].This modeling has also attracted the interest in biomedical applications in live sciences, such as: the use of stents to repair the endovascular [14, 20], the simulation of Minimally Invasive Surgery in which guidewires are inserted through the patient tissue with limited visual aids [9, 10] and the study of deformations and supercoiling phenomena of fragments of the DNA molecule where this study and the mechanical explanation of the phenomenon can help to produce and/or improve drugs for genetic diseases [12, 18]. Many problems that remain to be studied for a good understanding of the supercoiling process of DNA fragments, which are based on the modeling and numerical treatment of frictional or frictionless self-contact in elastic rods.

Contact problems seem to be among difficult to be treated both analytically and numerically. However, the techniques that take into account unilateral contact conditions are well advanced with the remarkable progress of computing machines. These techniques, which have solved these problems, are still need to be examined in return, especially the problem of self-contact. The unilateral contact problem with non-local Coulomb friction has been studied by Renard [23]. For static and dynamic unilateral contact problems with Coulomb friction, where the existence and/or uniqueness of solutions for discretized problems have been proved, we can refer to [6].

Key roles in studying the self-contact problem in an elastic rod or rod to rod contact are how these structures react when they suffer contact forces. A new three-stages contact searching algorithm based on bounding volume hierarchies and orthogonal projections for a frictional self-contact problem between rope fibers in the large deformations case has developed by Peng et al. [21]. About the modeling of the frictionless contact between two rods in large displacements, where the existence of a static solution has been proved, we can cite [4]. The frictionless self-contact problem in elastic rods has been studied by Chamekh et al. [7] and recently by Bozorgmehri et al. [2], who gave an existence result based on a nonlinear minimization problem and numerical examples based on the complementarity problem (CP), the linear complementarity problem (LCP), the penalty and augmented Lagrangian approaches.

The modeling of elastic rods with tangential self-friction was studied by Chamekh et al. [8] and well detailed in the thesis of Latrach [17]. The present work expands this modeling to the rotational self-friction case, where the great unexpected difficulty (theoretically) is to prove the existence of solutions to the theoretical problem of finding the equilibrium configurations like the tangential self-friction case, let us note that sometimes the mathematical tools at our disposal cannot solve some problems because of their strong nonlinearity like

this example where the mathematical models used in themselves are nonlinear and lead to systems of nonlinear equations.

1.1 Assumptions and notations used

Throughout this report, we recall that the antisymmetric tensor $\boldsymbol{a}^{\times} = skew(\boldsymbol{a})$ associated with the vector $\boldsymbol{a} \in \mathbb{R}^3$ is defined by $\boldsymbol{a}^{\times}\boldsymbol{b} = \boldsymbol{a} \times \boldsymbol{b}$ for all $\boldsymbol{b} \in \mathbb{R}^3$, and

$$P_{B(\tau)}[\boldsymbol{a}] = \begin{cases} \boldsymbol{a} & \text{if } \|\boldsymbol{a}\| < \tau, \\ \tau \frac{\boldsymbol{a}}{\|\boldsymbol{a}\|} & \text{otherwise,} \end{cases}$$

is the projection of the vector $\boldsymbol{a} \in \mathbb{R}^3$ onto the centered ball at the origin and with a radius τ. For any function G differentiation with respect to the curvilinear abscissa is denoted with prime ($G' = \dfrac{\partial G}{\partial s}$) and with respect to the time is denoted with dot ($\dot{G} = \dfrac{\partial G}{\partial t}$). Time discretization is based on a backward Euler approximation of the last notation which reads, see [19]

$$\dot{G}(s) = \frac{G(s) - G(s_0)}{\Delta t} \tag{1.1}$$

2 Cosserat rod

2.1 A 3-D curved Cosserat rod

We make use in this paper the geometrically exact theory of rods which is largely based on the model introduced by Cosserat brothers [5]. This model is used in the abstract framework proposed by Antman [1] and developed in [22, 25]. More recently, Chamekh et al. [8] has treated the frictional self-contact problem of elastic rods in the case of tangential friction only. We will extend this study to the rotational self-friction case.

Let $\mathcal{R}$ an elastic rod with the length l defined by a regular set of cross sections $\{A(s)$ [1]; $s \in [0; l]\}$ and fixed on the spatial basis $(\boldsymbol{e}_i)_i$. The cross sections are circular of uniform diameter 2ε. In [8], the authors presented the different configurations of the rod. Within this framework, the deformed configuration, under the action of external efforts, can be completely determined by the position vector $\boldsymbol{r} \in \mathbb{R}^3$ and the orthogonal tensor $\boldsymbol{R} = \boldsymbol{d}_i \otimes \boldsymbol{e}_i \in SO(3)$, with $SO(3)$ is the group of rotation matrices in $\mathbb{R}^3$. The orthogonal tensor $\boldsymbol{R}$ is the matrix which associates with the spatial basis $(\boldsymbol{e}_i)_i$ the material basis $(\boldsymbol{d}_i)_i$. The position vector $\boldsymbol{r}_0$ and the tensor $\boldsymbol{R}_0 = \boldsymbol{d}_{0i} \otimes \boldsymbol{e}_i$ are associated with the stress-free configuration, see Fig. 1. The Kinematics of deformation of a Cosserat elastic rod is detailed in the thesis of Latrach [17].

[1] $A(s)$ is the adherence of a bounded open set of $\mathbb{R}^2$ which contains 0 for all $s \in [0; l]$ and which will serve to describe the "$form$" and "$size$" of cross-sections of the rod.

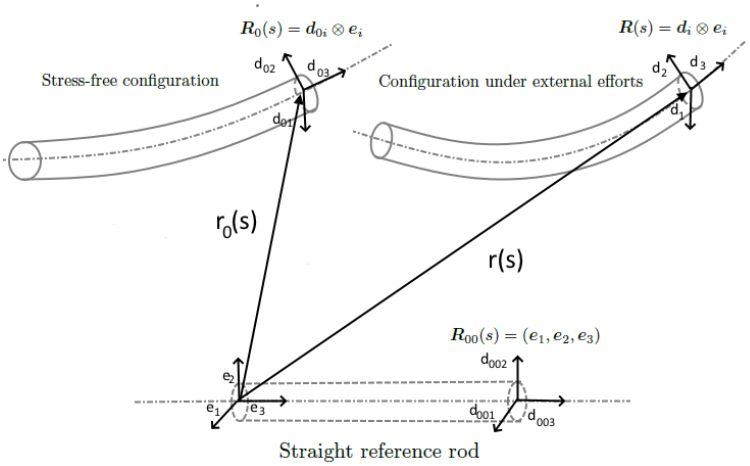

Fig. 1 3-D configurations of a Cosserat elastic rod.

2.2 Strains Measures and mechanical interpretation

The rotation tensor $\boldsymbol{R}$ may be expressed by the well-known Euler-Rodrigues formula

$$\boldsymbol{R} = \boldsymbol{I_3} + \sin(\theta)\boldsymbol{\omega}^{\times} + [1 - \cos(\theta)](\boldsymbol{\omega}^{\times})^2, \tag{2.1}$$

in which $\boldsymbol{\theta} = \theta\boldsymbol{\omega}$ is the Euler rotation vector. We use the Taylor series for $\sin(\theta)$ and $\cos(\theta)$ and the relations $(\boldsymbol{\omega}^{\times})^{2n+1} = (-1)^n\boldsymbol{\omega}^{\times}$ and $(\boldsymbol{\omega}^{\times})^{2n} = (-1)^{n-1}(\boldsymbol{\omega}^{\times})^2$, we obtain the exponential form of $\boldsymbol{R}$

$$\boldsymbol{R} = \boldsymbol{I_3} + \frac{[\theta\boldsymbol{\omega}^{\times}]}{1!} + \frac{[\theta\boldsymbol{\omega}^{\times}]^2}{2!} + \frac{[\theta\boldsymbol{\omega}^{\times}]^3}{3!} + \cdots = \exp[\boldsymbol{\theta}^{\times}]. \tag{2.2}$$

The vector $\boldsymbol{\theta}'$ is exactly the vector $\boldsymbol{u}$ defined in [8], i.e. $\boldsymbol{\theta}' \times \boldsymbol{d}_i = \boldsymbol{u} \times \boldsymbol{d}_i = \boldsymbol{d}_i'$. Following [1], we introduce the measures of deformation:

$$\mathbf{v} = \boldsymbol{R}^T\boldsymbol{r}' \quad \text{and} \quad \mathbf{u} = \boldsymbol{R}^T\boldsymbol{\theta}'. \tag{2.3}$$

With $\mathbf{v}$ is a translational deformations vector, which its components v_3 measure the elongation and v_1 and v_2 measure the shear deformations, respectively, in the $\boldsymbol{d}_1$ and $\boldsymbol{d}_2$ directions. The components of vector $\mathbf{u}$, are u_1 and u_2 that measure the total flexion of the rod, respectively, in the planes $(\boldsymbol{d}_2, \boldsymbol{d}_3)$ and $(\boldsymbol{d}_1, \boldsymbol{d}_3)$ and u_3 that is a measure of the total physical twist of the rod around the vector $\boldsymbol{d}_3$.

3 Self-contact with Coulomb friction

Our aim is to describe the two types of self-friction in an elastic rod such as the rotational self-friction. In [7], the authors have made a rigorous mathematical

analysis of the frictionless self-contact problem. Recently, we have presented the tangential self-friction problem in [8].

3.1 Self-contact problem

The maximum curvature condition of the rod expressing the fact that for each curvilinear abscissa $s \in [0, l]$, there exist a subset $\mathcal{I}_s$ of [0,l] of the points likely to come into contact with s. Note that $\mathcal{I}_s$ determined by a strictly positive constant which is selected according to the rigidity and the regular size of the cross-sections of the rod, see Fig. 2.

In the deformed configuration, as the curve $\boldsymbol{r}([0, l])$ is continuous and the subset $\mathcal{I}_s$ is compact, the research of the point of contact with $\boldsymbol{r}(s)$ can result in finding the orthogonal projection $\boldsymbol{r}(\bar{s}) \in \boldsymbol{r}(\mathcal{I}_s)$ of $\boldsymbol{r}(s)$. We can therefore write

$$\boldsymbol{r}'(\bar{s}) \cdot (\boldsymbol{r}(s) - \boldsymbol{r}(\bar{s})) = 0. \tag{3.1}$$

We can also define $\bar{s}$ by the arclength of the closest point to s, i.e. $\bar{s} = \operatorname{argmin}_{\sigma \in \mathcal{I}_s} \|\boldsymbol{r}(s) - \boldsymbol{r}(\sigma)\|$.

The evident self-impenetrability condition expressing the fact the volumes cannot interpenetrate themselves in a kinematically and physically admissible configuration of the rod. Consequently, for a given configuration of the rod we define a *gap function* with their imposed constraint

$$d_{\boldsymbol{r}}(s, \bar{s}) = 2\varepsilon - \|\boldsymbol{r}(s) - \boldsymbol{r}(\bar{s})\| \leq 0, \quad \forall s \in [0, l]. \tag{3.2}$$

The true self-contact distance must be dependent on both the position vector $\boldsymbol{r}(s)$ and the rotation tensor $\boldsymbol{R}(s)$ because it must be defined with respect the cross-section boundarie $A(s)$ and the lateral surface of $\{A(\sigma),\ \sigma \in \mathcal{I}_s\}$. The determination of the true distance of contact could be quite complicated. Thus, $d_{\boldsymbol{r}}$ is defined as an approximation to the true self-contact distance (*gap function*) such that the associated *gap vector* is given by

$$\boldsymbol{D}_{\boldsymbol{r}}(s, \bar{s}) = -d_{\boldsymbol{r}}(s, \bar{s}) \boldsymbol{N}(s, \bar{s}), \tag{3.3}$$

According to (3.1), $\boldsymbol{N}$ is the unit normal vector orthogonal to $\boldsymbol{T}(s, \bar{s})$ the tangent vector to the center line of the rod at arclength $\bar{s}$:

$$\boldsymbol{N}(s, \bar{s}) = \frac{\boldsymbol{r}(s) - \boldsymbol{r}(\bar{s})}{\|\boldsymbol{r}(s) - \boldsymbol{r}(\bar{s})\|}, \qquad \text{and} \quad \boldsymbol{T}(s, \bar{s}) = \frac{\boldsymbol{r}'(\bar{s})}{\|\boldsymbol{r}'(\bar{s})\|}.$$

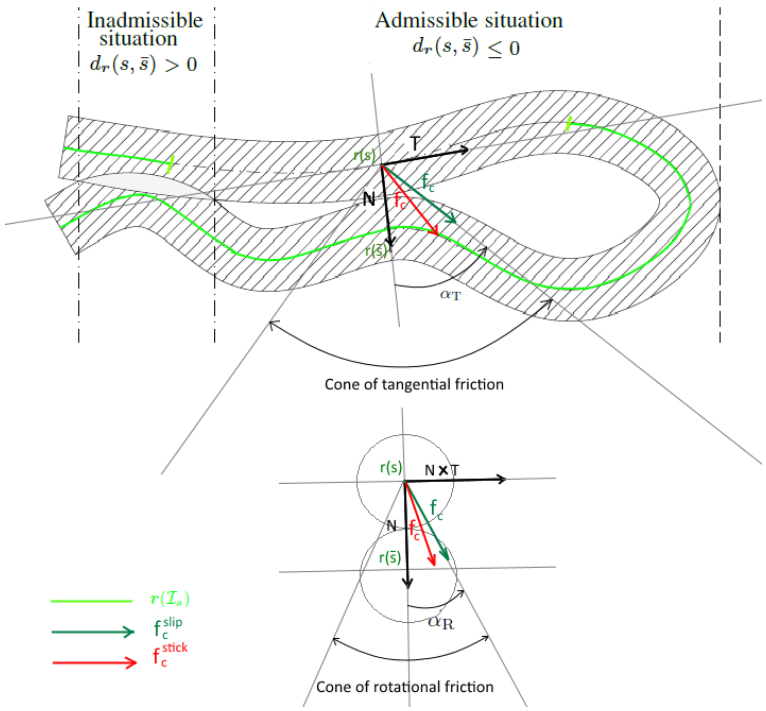

Fig. 2 Geometric modeling of an elastic rod with Coulomb friction

3.2 Modeling of tangential and rotational self-friction

The constraint of the self-impenetrability in (3.2) can be expressed in terms of a contact force. Under the assumption of frictional self-contact, this force must be decomposed to a normal pressure and two frictional efforts (tangential and rotational forces). In this paper, the Cosserat model is based on the central curve of the rod, whereas the contact force must be mechanically defined as a force applied by the point $\boldsymbol{r}(s)$ on a point of a compact 3D-neighborhood of $\boldsymbol{r}(\bar{s})$ defined by the friction cone, see Fig. 2.

$$\boldsymbol{f}_c(s) = f_{\mathrm{N}}(s)\boldsymbol{N}(s,\bar{s}) + \boldsymbol{f}_{\mathrm{T}}(s) + \boldsymbol{f}_{\mathrm{R}}(s).$$

With the internal production of this force and under the action of external forces $\boldsymbol{f}_{\mathrm{ext}}$ and external torques $\boldsymbol{t}_{\mathrm{ext}}$, the local form of the balance equations for a rod can be written in the following way:

$$\boldsymbol{n}' + \boldsymbol{f}_{\mathrm{ext}} + \boldsymbol{f}_N\boldsymbol{N} + \boldsymbol{f}_T = \boldsymbol{0} \quad \text{and} \quad \boldsymbol{m}' + \boldsymbol{r}'\times\boldsymbol{n} + \boldsymbol{t}_{\mathrm{ext}} + \boldsymbol{f}_R = \boldsymbol{0}, \qquad (3.4)$$

where $\boldsymbol{n}$ and $\boldsymbol{m}$ denote respectively resultant force (of the material with $\sigma > s$ on the material with $\sigma < s$) and resultant moments acting across the cross-section $A(\boldsymbol{r}(s))$.

The rod model studied in this paper is supposed to be made of a hyperelastic material, i.e. there exists an elastic energy density $\mathcal{W}(\cdot, \mathbf{u}, \mathbf{v})$ such that:

$$\boldsymbol{n} = \boldsymbol{R}\frac{\partial \mathcal{W}(\cdot, \mathbf{u}, \mathbf{v})}{\partial \mathbf{v}} \quad \text{and} \quad \boldsymbol{m} = \boldsymbol{R}\frac{\partial \mathcal{W}(\cdot, \mathbf{u}, \mathbf{v})}{\partial \mathbf{u}}. \tag{3.5}$$

The elastic energy density $\mathcal{W}(s, \mathbf{u}, \mathbf{v})$ is supposed obeys the convexity and coercivity hypotheses with respect to its last two arguments.

The constraint of the self-impenetrability is gained the following Kuhn-Tucker conditions:

$$d_{\boldsymbol{r}}(s, \bar{s}) \leq 0, \quad f_{\mathrm{N}}(s) \geq 0 \quad \text{and} \quad d_{\boldsymbol{r}}(s, \bar{s}) f_{\mathrm{N}}(s) = 0. \tag{3.6}$$

In what follows, we assume that the sliding is persistent, i.e. if $d_{\boldsymbol{r}}(s, \bar{s}) = 0$, then $\dot{d}_{\boldsymbol{r}}(s, \bar{s}) = 0$.

To model the self-friction, it is necessary to determine the tangential and rotational sliding velocities which will make it possible to evaluate the pressure of the frictional efforts. The rotational sliding must be carried out on the cross-section boundarie $A(\bar{s})$ and around the $\boldsymbol{d}_3(\bar{s})$-axis while the tangential sliding must be carried out on the plane tangent and orthogonal to the cross-section $A(\bar{s})$. The tangential sliding velocity is given by (see [8]):

$$\boldsymbol{g}_{\boldsymbol{r}}(s, \bar{s}) = \dot{\boldsymbol{r}}(s) - \dot{\boldsymbol{r}}(\bar{s}) + 2\varepsilon \dot{\boldsymbol{N}}(s, \bar{s}). \tag{3.7}$$

The tangential sticking can be defined as follows:

- if $\boldsymbol{g}_{\boldsymbol{r}}(s, \bar{s}) = \mathbf{0}$ then the curve is a tangentially self-sticking;
- if $\boldsymbol{g}_{\boldsymbol{r}}(s, \bar{s}) \neq \mathbf{0}$ then the curve is a tangentially self-sliding.

By differentiation with respect to time in (2.2) we obtain

$$\begin{aligned} \dot{\boldsymbol{d}}_i(s) &= \dot{\boldsymbol{\theta}}(s) \times \boldsymbol{d}_i(s), \\ \dot{\boldsymbol{d}}_i(\bar{s}) &= [\dot{\boldsymbol{\theta}}(\bar{s}) + \dot{\bar{s}}\boldsymbol{\theta}'(\bar{s})] \times \boldsymbol{d}_i(\bar{s}). \end{aligned}$$

Then, we consider the following rotational sliding velocity

$$\boldsymbol{g}_{\boldsymbol{R}}(s, \bar{s}) = \dot{\boldsymbol{\theta}}(s) - \dot{\boldsymbol{\theta}}(\bar{s}) - \dot{\bar{s}}\boldsymbol{\theta}'(\bar{s}). \tag{3.9}$$

The rotational sticking can be defined as follows:

- if $\boldsymbol{g}_{\boldsymbol{R}}(s, \bar{s}) = \mathbf{0}$, rotation along the $\boldsymbol{d}_3(\bar{s})$-axis is not possible.
- if $\boldsymbol{g}_{\boldsymbol{R}}(s, \bar{s}) \neq \mathbf{0}$, can be rotated along the $\boldsymbol{d}_3(\bar{s})$-axis.

3.3 Coulomb's law

The simplest (in appearance) is Tresca's law, it has been successfully implanted in many works. But, the conditions of Trisca friction do not really make sense in greater deformations case because the self-penetration is possible and they also impose a little friction even before self-contact, which is obviously not at all physically. Thus, friction is generally taken into account using Coulomb's law, that is relevant for a broad range of applications. In the following, one will count on Coulomb's law to discuss the problem of self-friction in elastic rod:

$$\|\boldsymbol{f}_{\mathrm{T}}(s)\| < \gamma_{\mathrm{T}} f_{\mathrm{N}}(s) \qquad \text{if} \quad \boldsymbol{g_r}(s,\bar{s}) = \boldsymbol{0}, \tag{3.10a}$$

$$\boldsymbol{f}_{\mathrm{T}}(s) = \gamma_{\mathrm{T}} f_{\mathrm{N}}(s) \frac{\boldsymbol{g_r}(s,\bar{s})}{\|\boldsymbol{g_r}(s,\bar{s})\|} \qquad \text{otherwise}, \tag{3.10b}$$

$$\|\boldsymbol{f}_{\mathrm{R}}(s)\| < \gamma_{\mathrm{R}} f_{\mathrm{N}}(s) \qquad \text{if} \quad \boldsymbol{g_R}(s,\bar{s}) = \boldsymbol{0}, \tag{3.10c}$$

$$\boldsymbol{f}_{\mathrm{R}}(s) = \gamma_{\mathrm{R}} f_{\mathrm{N}}(s) \frac{\boldsymbol{g_R}(s,\bar{s})}{\|\boldsymbol{g_R}(s,\bar{s})\|} \qquad \text{otherwise.} \tag{3.10d}$$

Here, γ_{T} and γ_{R} are respectively the tangential and rotational friction coefficients for the master point which are generally constant depending on the reality of the materials and the environments considered (surface states, temperature, tangential sliding speed, ...). The inequalities and equality (3.6) express the condition of non-self-penetration of matter and the fact that the normal contact stress is of compression which must be zero as well as the tangential and rotational stress if there is no self-contact (3.10a,3.10c). The tangential and rotational efforts of Coulomb friction cannot exceed the positive thresholds given by $\gamma_{\mathrm{T}} f_{\mathrm{N}}$ and $\gamma_{\mathrm{R}} f_{\mathrm{N}}$ which is translated into the friction conditions (3.10) by the fact that if the tangential or rotational stress of the contact force reaches the given threshold, then there is a tangential or rotational self-sliding, else there is a tangential or rotational self-sticking. In other words, the tangential and rotational friction cones, respectively, defined by the angles $\alpha_{\mathrm{T}} = \arctan(\gamma_{\mathrm{T}})$ and $\alpha_{\mathrm{R}} = \arctan(\gamma_{\mathrm{R}})$ decide whether there is a slip or not, see Fig.2

4 Principle of virtual work of the self-friction problem

We couldn't offer an expression of the total energy of an elastic rod subjected to external forces in the presence of friction because the frictional Coulomb's law does not admit of potential. For this reason, we will directly present a weak variational formulation approach associated with equations (3.4) describing the equilibrium states of a hyperelastic rod. In this approach, we will adopt the augmented Lagrangian method and the approximations used in [8] to present a global approximation of the principle of virtual work, taking into

account the constraint of self-impenetrability:

$$\begin{aligned}\mathcal{G}(\boldsymbol{r},\boldsymbol{\theta};\delta\boldsymbol{r},\delta\boldsymbol{\theta}) &= \int_0^l \left\{\boldsymbol{n}(s)\cdot\left(\delta\boldsymbol{r}'(s)-\delta\boldsymbol{\theta}(s)\times\boldsymbol{r}'(s)\right)+\boldsymbol{m}(s)\cdot\delta\boldsymbol{\theta}'(s)\right\}\,ds\\ &\quad-\int_0^l\left\{\boldsymbol{f}_{\text{ext}}(s)\cdot\delta\boldsymbol{r}(s)+\boldsymbol{t}_{\text{ext}}\cdot\delta\boldsymbol{\theta}(s)\right\}\,ds\\ &\quad+\int_0^l\left\{(f_{\text{N}}^{\mu_{\text{N}}}(s)\boldsymbol{N}(s,\bar{s})+\boldsymbol{f}_{\text{T}}^{\mu_{\text{T}}}(s))\cdot(\delta\boldsymbol{r}(\bar{s})-\delta\boldsymbol{r}(s))\right\}\,ds\\ &\quad+\int_0^l\left\{\boldsymbol{f}_{\text{R}}^{\mu_{\text{R}}}(s)\cdot(\delta\boldsymbol{\theta}(\bar{s})-\delta\boldsymbol{\theta}(s))\right\}\,ds\\ &=\mathbf{0}.\end{aligned}\tag{4.1}$$

The first two integral parts represent the virtual work of internal forces and external loads, and the last two integral parts represent an approach of virtual work of self-friction force given by the following triple:

$$f_{\text{N}}^{\mu_{\text{N}}}(s)=\frac{1}{\mu_{\text{N}}}\left[d_{\boldsymbol{r}}(s,\bar{s})+\mu_{\text{N}}\lambda_{\text{N}}^n(s)\right]_+,\qquad [x]_+=\frac{1}{2}(x+|x|),\tag{4.2a}$$

$$\boldsymbol{f}_{\text{T}}^{\mu_{\text{T}}}(s)=\frac{1}{\mu_{\text{T}}}P_{B_{\text{T}}}\left[\boldsymbol{g}_{\boldsymbol{r}}(s,\bar{s})+\mu_{\text{T}}\boldsymbol{\lambda}_{\text{T}}^n(s)\right],\qquad B_{\text{T}}=B(\mu_{\text{T}}\gamma_{\text{T}}f_{\text{N}}^{\mu_{\text{N}}}),\tag{4.2b}$$

$$\boldsymbol{f}_{\text{R}}^{\mu_{\text{R}}}(s)=\frac{1}{\mu_{\text{R}}}P_{B_{\text{R}}}\left[\boldsymbol{g}_{\boldsymbol{R}}(s,\bar{s})+\mu_{\text{R}}\boldsymbol{\lambda}_{\text{R}}^n(s)\right],\qquad B_{\text{R}}=B(\mu_{\text{R}}\gamma_{\text{R}}f_{\text{N}}^{\mu_{\text{N}}}),\tag{4.2c}$$

where μ_{N}, μ_{T} and μ_{R} are the normal, tangential and rotational penalties parameters, and the iterative approaches $\lambda_{\text{N}}^n(s)$, $\boldsymbol{\lambda}_{\text{T}}^n(s)$ and $\boldsymbol{\lambda}_{\text{R}}^n(s)$ are updated according to iterations used in [8]. Thereby, the problem of finding the equilibrium configurations that satisfy the equilibrium equations (3.4) leads to the following nonlinear penalized problem

$$\begin{cases}\text{Find } (\boldsymbol{r},\boldsymbol{\theta})\in\mathcal{C} \text{ such that}\\ \mathcal{G}(\boldsymbol{r},\boldsymbol{\theta};\delta\boldsymbol{r},\delta\boldsymbol{\theta})=0,\quad\forall(\delta\boldsymbol{r},\delta\boldsymbol{\theta}),\end{cases}\tag{4.3}$$

the set $\mathcal{C}$ being given by

$$\mathcal{C}=\left\{(\boldsymbol{r},\boldsymbol{\theta})\in H^1([0,l];\mathbb{R}^3\times\mathbb{R}^3),\quad \boldsymbol{r}(0)=\mathbf{0},\quad \boldsymbol{\theta}(0)=\boldsymbol{\theta}^0,\quad \boldsymbol{\theta}(l)=\boldsymbol{\theta}^l\right\}.$$

Remark 41 *As in [8], the self-friction force given by* (4.2) *is equivalent to the Kuhn-Tucker and the self-friction conditions* (3.6) *and* (3.10)*. Then, the augmented Lagrangian method reassures us about the self-contact conditions.*

5 Existence of solution for the penalized formulation

If $\boldsymbol{f}$ is independent of $\boldsymbol{r}$, then the problem of finding the equilibrium configurations that satisfy the equilibrium equations (3.4) with the penalized frictional self-contact force (4.2) and the constitutive laws (3.5) leads to the following nonlinear approximated minimization problem

$$\begin{cases} \text{Find } (\boldsymbol{r}_\mu^n, \boldsymbol{\theta}_\mu^n) \in \mathcal{C} \text{ such that} \\ \mathcal{J}_\mu^n(\boldsymbol{r}_\mu^n, \boldsymbol{\theta}_\mu^n) \leq \mathcal{J}_\mu^n(\boldsymbol{q}, \boldsymbol{\varphi}) \quad \forall (\boldsymbol{q}, \boldsymbol{\varphi}) \in \mathcal{C}, \end{cases} \tag{5.1}$$

where (4.1) is the necessary condition for minimizing the above total energy with the same normal, tangential and rotational penalties parameters (they are equal to μ).

In this paper, for the sake of simplicity, we shall assume that the rod is not subject to distributed torque $\boldsymbol{t}_{\text{ext}} = \boldsymbol{0}$. Then, the energy expression $\mathcal{J}_\mu^n$ for an elastic rod in balance is given by

$$\mathcal{J}_\mu^n(\boldsymbol{r}, \boldsymbol{\theta}) = \int_0^l \left[\mathcal{W}(s, \mathbf{v}, \mathbf{u}) - \boldsymbol{f} \cdot \boldsymbol{r} - \left(\lambda_N^n \boldsymbol{N}^\varepsilon + \boldsymbol{\lambda}_T^{n,\mu} \right) \cdot \boldsymbol{r} - \boldsymbol{\lambda}_R^{n,\mu} \cdot \boldsymbol{\theta} \right] ds, \tag{5.2}$$

where $\lambda_N^n \boldsymbol{N}^\varepsilon$, $\boldsymbol{\lambda}_T^{n,\mu}$ and $\boldsymbol{\lambda}_R^{n,\mu}$ are the Lagrange multipliers given in (4.2) with the next regularizations to ensure that the self-contact force fields belong to the space $L^2([0,l];\mathbb{R}^3)$:

$$\boldsymbol{N}^\varepsilon = \begin{cases} \frac{\boldsymbol{r}(s) - \boldsymbol{r}(\bar{s})}{2\varepsilon} & \text{if} \quad \|\boldsymbol{r}(s) - \boldsymbol{r}(\bar{s})\| \leq 2\varepsilon, \\ \frac{\boldsymbol{r}(s) - \boldsymbol{r}(\bar{s})}{\|\boldsymbol{r}(s) - \boldsymbol{r}(\bar{s})\|} & \text{otherwise,} \end{cases}$$

if $\|\boldsymbol{g}_r + \mu\| \boldsymbol{\lambda}_{\mathrm{T}}^{n,\mu} \geq \mu \gamma_T \lambda_N^n$:

$$\boldsymbol{\lambda}_T^{n,\mu} = \begin{cases} \gamma_T \lambda_N^n \ \frac{\boldsymbol{g}_r + \mu \boldsymbol{\lambda}_{\mathrm{T}}^{n,\mu}}{\mu} & \text{elseif} \quad \left\| \boldsymbol{g}_r + \mu \boldsymbol{\lambda}_{\mathrm{T}}^{n,\mu} \right\| \leq \mu, \\ \gamma_T \lambda_N^n \ \frac{\boldsymbol{g}_r + \mu \boldsymbol{\lambda}_{\mathrm{T}}^{n,\mu}}{\left\| \boldsymbol{g}_r + \mu \boldsymbol{\lambda}_{\mathrm{T}}^{n,\mu} \right\|} & \text{otherwise,} \end{cases}$$

if $\left\| \boldsymbol{g}_R + \mu \boldsymbol{\lambda}_{\mathrm{R}}^{n,\mu} \right\| \geq \mu \gamma_R \lambda_N^n$:

$$\boldsymbol{\lambda}_R^{n,\mu} = \begin{cases} \gamma_R \lambda_N^n \ \frac{\boldsymbol{g}_R + \mu \boldsymbol{\lambda}_{\mathrm{R}}^{n,\mu}}{\mu} & \text{elseif} \quad \left\| \boldsymbol{g}_R + \mu \boldsymbol{\lambda}_{\mathrm{R}}^{n,\mu} \right\| \leq \mu, \\ \gamma_R \lambda_N^n \ \frac{\boldsymbol{g}_R + \mu \boldsymbol{\lambda}_{\mathrm{R}}^{n,\mu}}{\left\| \boldsymbol{g}_R + \mu \boldsymbol{\lambda}_{\mathrm{R}}^{n,\mu} \right\|} & \text{otherwise.} \end{cases}$$

The function $\mathcal{W}$ that appeared in (5.2) is a typical example for the elastic stored energy functional: $\mathcal{W}(\cdot, \mathbf{u}, \mathbf{v}) = \frac{1}{2} \mathbf{w}^T \boldsymbol{A} \mathbf{w}$, where $\boldsymbol{A}(s) \in \boldsymbol{M}_6(\mathbb{R})$ is a coercive, symmetric and positive-definite matrix and $\mathbf{w}^T = (\mathbf{u}^T, \mathbf{v}^T)$.

Theorem 51 *Let us assume that the external force $\boldsymbol{f}$ is in $L^2([0,l];\mathbb{R}^3)$, then for each $n \in \mathbb{N}$ and $\mu \in]0,1[$, the problem* (5.1) *with the energy functional* (5.2) *has at least one solution.*

Proof. The proof of the theorem is based on the generalized Weierstrass theorem [15], That is to say, it must be prove on the one hand that the energy functional (5.2) is weakly lower semicontinuous and coercive, and on the other hand that the set $\mathcal{C}$ is sequentially weakly closed in $H^1([0,l];\mathbb{R}^3\times\mathbb{R}^3)$.

The mapping

$$(\mathbf{u},\mathbf{v})\in L^2([0,l];\mathbb{R}^3\times\mathbb{R}^3)\mapsto\int_0^l\mathcal{W}(s,\mathbf{v},\mathbf{u})ds,$$

is convex and continuous, and hence weakly lower semicontinuous over $L^2([0,l];\mathbb{R}^3\times\mathbb{R}^3)$ because, $\mathcal{W}(s,\cdot,\cdot)$ is convex and quadratic with bounded coefficients. Furthermore, the mapping

$$(\boldsymbol{r},\boldsymbol{\theta})\in H^1([0,l];\mathbb{R}^3\times\mathbb{R}^3)\mapsto(\mathbf{u},\mathbf{v})=(\boldsymbol{R}^T\boldsymbol{r}',\boldsymbol{R}^T\boldsymbol{\theta}')\in L^2([0,l];\mathbb{R}^3\times\mathbb{R}^3),$$

is weakly continuous, we therefore deduce that the function

$$(\boldsymbol{r},\boldsymbol{\theta})\in H^1([0,l];\mathbb{R}^3\times\mathbb{R}^3)\mapsto\int_0^l\mathcal{W}(s,\mathbf{v},\mathbf{u})ds\in\mathbb{R},$$

is convex and weakly lower semicontinuous over $H^1([0,l];\mathbb{R}^3\times\mathbb{R}^3)$. Since the penalized self-contact force fields belong to the space $L^2([0,l];\mathbb{R}^3)$, the mapping

$$(\boldsymbol{r},\boldsymbol{\theta})\in H^1([0,l];\mathbb{R}^3\times\mathbb{R}^3)\mapsto\int_0^l\left[\left(\lambda_N^n\boldsymbol{N}^\varepsilon+\boldsymbol{\lambda}_T^{n,\mu}\right)\cdot\boldsymbol{r}+\boldsymbol{\lambda}_R^{n,\mu}\cdot\boldsymbol{\theta}\right]ds\in\mathbb{R}_+,$$

is convex and hence weakly lower semicontinuous. Therefore, the energy functional $\mathcal{J}_\mu^n$ is weakly lower semicontinuous over $H^1([0,l];\mathbb{R}^3\times\mathbb{R}^3)$.

As in [8], there exist constant c_1, c_2, c_3 and c_4 such that

$$\mathcal{J}_\mu^n(\boldsymbol{r},\boldsymbol{\theta})\geq c_1\|\boldsymbol{r}\|_{1,2}^2+\frac{c_2}{2}\left[\,\|\boldsymbol{\theta}\|_{1,2}^2-l\,\right]-\left[\,\|\boldsymbol{f}\|_2+\lambda_N^n\|\boldsymbol{N}^\varepsilon\|_2+\|\boldsymbol{\lambda}_T^{n,\mu}\|_2\,\right]\|\boldsymbol{r}\|_{1,2}-\|\boldsymbol{\lambda}_R^{n,\mu}\|_2\|\boldsymbol{\theta}\|_{1,2}.$$

where $\|\cdot\|_{1,2}$ denotes the usual norm in $H^1([0,l];\mathbb{R}^3)$. Therefore the functional $\mathcal{J}_\mu^n$ is coercive.

The weak closure of the set $\mathcal{C}$ is proved in [3] which ends the proof. □

6 Linearization of virtual work equation

To solve the nonlinear problem (4.3) we propose the Newton-Raphson method, this method is based on the linearization of each term of the formulation (4.1) to solve the following linearized problem

$$\mathcal{G}(\boldsymbol{r}^k,\boldsymbol{R}^k;\delta\boldsymbol{r},\delta\boldsymbol{\theta})+\Delta\mathcal{G}(\boldsymbol{r}^k,\boldsymbol{R}^k;\delta\boldsymbol{r},\delta\boldsymbol{\theta};\boldsymbol{\eta},\boldsymbol{\vartheta})=0,\tag{6.1}$$

where the symbol Δ denotes the directional derivative defined by

$$\Delta\mathcal{G}(\boldsymbol{r}^k,\boldsymbol{R}^k;\delta\boldsymbol{r},\delta\boldsymbol{\theta};\boldsymbol{\eta},\boldsymbol{\vartheta}):=\left.\frac{d}{d\epsilon}\right|_{\epsilon=0}\mathcal{G}(\boldsymbol{r}^k+\epsilon\boldsymbol{\eta},\exp(\epsilon\boldsymbol{\vartheta}^\times)\boldsymbol{R}^k;\delta\boldsymbol{r},\delta\boldsymbol{\theta}).$$

The Newton update scheme of the displacement $\boldsymbol{r}$ is additive $\boldsymbol{r}^{k+1} = \boldsymbol{r}^k + \boldsymbol{\eta}$ but, to updating the rotation $\boldsymbol{R}$ we use a multiplicative update $\boldsymbol{R}^{k+1} = \exp(\boldsymbol{\vartheta}^{\times})\boldsymbol{R}^k$.

The linearization of the virtual work of internal forces and moments (the first two integral parts in (4.1)) is presented by Chamekh et al. [7] of a rod not subject to distributed torque, i.e. $\boldsymbol{t}_{\text{ext}} = \boldsymbol{0}$. The linearizations of the virtual work associated with normal force and the virtual work associated with tangential effort (the third integral part in (4.1)) are respectively already made in [7] and [8].

In the next, we highlight more on the linearization of the virtual work of rotational self-friction force given by the fourth integral part in (4.1).

6.1 Linearization of the virtual work of rotational self-friction force

In view of (4.1), the virtual work of self-friction force is given by

$$\mathcal{G}_{\mathrm{c}}(\boldsymbol{r},\boldsymbol{\theta};\delta\boldsymbol{r},\delta\boldsymbol{\theta}) = \int_0^l \begin{pmatrix} f_{\mathrm{N}}^{\mu_{\mathrm{N}}}\boldsymbol{N} + \boldsymbol{f}_{\mathrm{T}}^{\mu_{\mathrm{T}}} \\ \boldsymbol{f}_{\mathrm{R}}^{\mu_{\mathrm{R}}} \end{pmatrix} \cdot \begin{pmatrix} \delta\boldsymbol{r}(\bar{s}) - \delta\boldsymbol{r}(s) \\ \delta\boldsymbol{\theta}(\bar{s}) - \delta\boldsymbol{\theta}(s) \end{pmatrix} ds. \tag{6.2}$$

Then, the directional derivative $\Delta\mathcal{G}_{\mathrm{c}}(\boldsymbol{r},\boldsymbol{\theta};\delta\boldsymbol{r},\delta\boldsymbol{\theta};\boldsymbol{\eta},\boldsymbol{\vartheta})$ is given by

$$\Delta\mathcal{G}_{\mathrm{c}} = \int_0^l \begin{pmatrix} \Delta f_{\mathrm{N}}^{\mu_{\mathrm{N}}}\boldsymbol{N} + f_{\mathrm{N}}^{\mu_{\mathrm{N}}}\Delta\boldsymbol{N} + \Delta\boldsymbol{f}_{\mathrm{T}}^{\mu_{\mathrm{T}}} \\ \Delta\bar{s}\big(f_{\mathrm{N}}^{\mu_{\mathrm{N}}}\boldsymbol{N} + \boldsymbol{f}_{\mathrm{T}}^{\mu_{\mathrm{T}}}\big) \\ \Delta\boldsymbol{f}_{\mathrm{R}}^{\mu_{\mathrm{R}}} \\ \Delta\bar{s}\boldsymbol{f}_{\mathrm{R}}^{\mu_{\mathrm{R}}} \end{pmatrix} \cdot \begin{pmatrix} \delta\boldsymbol{r}(\bar{s}) - \delta\boldsymbol{r}(s) \\ \delta\boldsymbol{r}'(\bar{s}) \\ \delta\boldsymbol{\theta}(\bar{s}) - \delta\boldsymbol{\theta}(s) \\ \delta\boldsymbol{\theta}'(\bar{s}) \end{pmatrix} ds. \tag{6.3}$$

The directional derivatives $f_{\mathrm{N}}^{\mu_{\mathrm{N}}}$, $\Delta\boldsymbol{f}_{\mathrm{T}}^{\mu_{\mathrm{T}}}$, $\Delta\boldsymbol{N}$ and $\Delta\bar{s}$ were calculated in [8], with notations $\bar{\boldsymbol{h}}(s) = \boldsymbol{h}(s) - \boldsymbol{h}(\bar{s})$ and $\breve{\boldsymbol{h}} = \boldsymbol{h}(\bar{s})$ for any vector-valued function $\boldsymbol{h}(\cdot)$, are given by

$$\Delta f_{\mathrm{N}}^{\mu_{\mathrm{N}}} = -\frac{1}{\mu_{\mathrm{N}}} H\big(d_{\boldsymbol{r}} + \mu_{\mathrm{N}}\lambda_{\mathrm{N}}^n\big)\bar{\boldsymbol{\eta}}\cdot\boldsymbol{N}, \tag{6.4a}$$

$$\Delta\boldsymbol{f}_{\mathrm{T}}^{\mu_{\mathrm{T}}} = \frac{F_T\big(\boldsymbol{g}_{\boldsymbol{r}} + \mu_{\mathrm{T}}\boldsymbol{\lambda}_{\mathrm{T}}^n\big)}{\mu_{\mathrm{T}}\Delta t}\big(\bar{\boldsymbol{\eta}} - \Delta\bar{s}\breve{\boldsymbol{r}}' + 2\varepsilon\Delta\boldsymbol{N}\big), \tag{6.4b}$$

$$\Delta\boldsymbol{N} = \frac{(\boldsymbol{I} - \boldsymbol{N}\otimes\boldsymbol{N})\bar{\boldsymbol{\eta}} - \Delta\bar{s}\breve{\boldsymbol{r}}'}{2\varepsilon - d_{\boldsymbol{r}}}, \tag{6.4c}$$

and, it follows from the directional derivative of (3.1) that the next equality gives an expression for $\Delta\bar{s}$

$$[\|\breve{\boldsymbol{r}}'\|^2 - \breve{\boldsymbol{r}}''\cdot\bar{\boldsymbol{r}}]\Delta\bar{s} = \bar{\boldsymbol{\eta}}\cdot\breve{\boldsymbol{r}}' + \bar{\boldsymbol{r}}\cdot\breve{\boldsymbol{\eta}}'. \tag{6.5}$$

The Heaviside function $H(x)$ in (6.4a) is equal to 1 if $x > 0$ and is equal to 0 if $x < 0$. The derivative is not defined at $x = 0$, a fact which we recognize but generally ignore in practice by taking $H(x)\,|_{x=0} = 1$. The function F_T in (6.4b) is defined by

$$F_{\mathrm{T}}(\boldsymbol{x}) = \begin{cases} 1 \text{ if } & \|\boldsymbol{x}\| \le \mu_{\mathrm{T}}\gamma_{\mathrm{T}} f_{\mathrm{N}}^{\mu_{\mathrm{N}}}, \\ 0 \text{ otherwise.} & \end{cases}$$

The similar function

$$F_{\mathrm{R}}(\boldsymbol{x}) = \begin{cases} 1 \text{ if } & \|\boldsymbol{x}\| \le \mu_{\mathrm{R}}\gamma_{\mathrm{R}} f_{\mathrm{N}}^{\mu_{\mathrm{N}}}, \\ 0 \text{ otherwise,} & \end{cases}$$

will appear in the directional derivative of $\boldsymbol{f}_{\mathrm{R}}^{\mu_{\mathrm{R}}}$ as follows

$$\begin{aligned} \Delta \boldsymbol{f}_{\mathrm{R}}^{\mu_{\mathrm{R}}} &= \Delta\{\frac{1}{\mu_{\mathrm{R}}} P_{B_{\mathrm{R}}^{n+1}}\big(\boldsymbol{g}_{\boldsymbol{R}} + \mu_{\mathrm{R}}\boldsymbol{\lambda}_{\mathrm{R}}^{n}\big)\} \\ &= \frac{1}{\mu_{\mathrm{R}}} \frac{\partial\big[P_{B_{\mathrm{R}}^{n+1}}\big(\boldsymbol{g}_{\boldsymbol{R}} + \mu_{\mathrm{R}}\boldsymbol{\lambda}_{\mathrm{R}}^{n}\big)\big]}{\partial \boldsymbol{g}_{\boldsymbol{R}}} \Delta \boldsymbol{g}_{\boldsymbol{R}} \\ &= \frac{1}{\mu_{\mathrm{R}}} F_R\big(\boldsymbol{g}_{\boldsymbol{R}} + \mu_{\mathrm{R}}\boldsymbol{\lambda}_{\mathrm{R}}^{n}\big) \Delta \boldsymbol{g}_{\boldsymbol{R}}. \end{aligned} \tag{6.6}$$

In view of the Euler approximation (1.1), the directional derivative of the rotational sliding velocity is given by

$$\Delta \boldsymbol{g}_{\boldsymbol{R}} = \frac{1}{\Delta t}\big[\bar{\boldsymbol{\vartheta}} - 2\Delta\bar{s}\breve{\boldsymbol{\theta}}' - (\bar{s} - \bar{s}_0)(\Delta\bar{s}\breve{\boldsymbol{\theta}}'' + \breve{\boldsymbol{\vartheta}}')\big]. \tag{6.7}$$

Upon substitution of (6.4), (6.5), (6.6) and (6.7) into (6.3), the final form of the directional derivative $\Delta\mathcal{G}_{\mathrm{c}}(\boldsymbol{r}, \boldsymbol{\theta}; \delta\boldsymbol{r}, \delta\boldsymbol{\theta}; \boldsymbol{\eta}, \boldsymbol{\vartheta})$ is given by

$$\begin{aligned} \Delta\mathcal{G}_{\mathrm{c}} = \int_0^l \Bigg[& \frac{H\big(d_{\boldsymbol{r}} + \mu_{\mathrm{N}}\lambda_{\mathrm{N}}^{n}\big)}{\mu_{\mathrm{N}}(2\varepsilon - d_{\boldsymbol{r}})} \boldsymbol{Q}_{\mathrm{N}} + \boldsymbol{Q}_{\mathrm{T}} + \frac{F_{\mathrm{T}}\big(\boldsymbol{g}_{\boldsymbol{r}} + \mu_{\mathrm{T}}\boldsymbol{\lambda}_{\mathrm{T}}^{n}\big)}{\mu_{\mathrm{T}}\Delta t(2\varepsilon - d_{\boldsymbol{r}})} \bar{\boldsymbol{\eta}} \cdot (2\varepsilon \boldsymbol{N}\otimes\boldsymbol{N} - d_{\boldsymbol{r}}\boldsymbol{I})\delta\bar{\boldsymbol{r}} \\ & + \boldsymbol{Q}_{\mathrm{R}} + \frac{F_{\mathrm{R}}\big(\boldsymbol{g}_{\boldsymbol{R}} + \mu_{\mathrm{R}}\boldsymbol{\lambda}_{\mathrm{R}}^{n}\big)}{\Delta t\mu_R}\big((\bar{s} - \bar{s}_0)\breve{\boldsymbol{\vartheta}}' \cdot \delta\bar{\theta} - \bar{\boldsymbol{\vartheta}} \cdot \delta\bar{\theta}\big)\Bigg]\, ds, \end{aligned} \tag{6.8}$$

with $\boldsymbol{Q}_{\mathrm{N}}$ and $\boldsymbol{Q}_{\mathrm{T}}$ are described respectively in [7] and [8], and $\boldsymbol{Q}_{\mathrm{R}}$ is given by

$$\boldsymbol{Q}_{\mathrm{R}} = \Omega \begin{pmatrix} \bar{\boldsymbol{\eta}} \\ \breve{\boldsymbol{\eta}}' \end{pmatrix} \cdot \begin{pmatrix} \Xi_{\mathrm{R}}\breve{\boldsymbol{r}}' \otimes (\breve{\boldsymbol{\theta}}' + \frac{\bar{s}-\bar{s}_0}{2}\breve{\boldsymbol{\theta}}'')\ \breve{\boldsymbol{r}}' \otimes \boldsymbol{f}_{\mathrm{R}}^{\mu_{\mathrm{R}}} \\ \Xi_{\mathrm{R}}\bar{\boldsymbol{r}} \otimes (\breve{\boldsymbol{\theta}}' + \frac{\bar{s}-\bar{s}_0}{2}\breve{\boldsymbol{\theta}}'')\ \ \bar{\boldsymbol{r}} \otimes \boldsymbol{f}_{\mathrm{R}}^{\mu_{\mathrm{R}}} \end{pmatrix} \begin{pmatrix} \delta\bar{\boldsymbol{\theta}} \\ \delta\breve{\boldsymbol{\theta}}' \end{pmatrix}$$

where

$$\Xi_{\mathrm{R}} = \frac{2F_{\mathrm{R}}\big(\boldsymbol{g}_{\boldsymbol{R}} + \mu_{\mathrm{R}}\boldsymbol{\lambda}_{\mathrm{R}}^{n}\big)}{\mu_{\mathrm{R}}\Delta t}, \quad \text{and} \quad \Omega = \frac{1}{\|\breve{\boldsymbol{r}}'\|^2 - \breve{\boldsymbol{r}}'' \cdot \bar{\boldsymbol{r}}}.$$

7 Finite-element implementation

We now proceed to give an finite-element implementation of the linearized frictional self-contact problem (6.1). Due to its generality and richness, the finite-element method has been used with remarkable success in solving a wide variety of problems in engineering fields. This method consists in dividing the domain of the solution into a finite number of subdomains and using the variational formulations to build an approximation of the solution on each

finite element. For this, we define a uniform subdivision of the interval $[0, l]$ into typical elements as follows

$$[0, l] = \bigcup_{e=1}^{N} I_h^e, \qquad h = \frac{l}{N}, \qquad I_h^e = [s_{e-1}, s_e].$$

where $N \in \mathbb{N}$ is the number of elements. Accordingly, we can approximate a field variable $\boldsymbol{g}$ (such as $\boldsymbol{r}$, $\boldsymbol{\theta}$, $\delta\boldsymbol{r}$, $\delta\boldsymbol{\theta}$, $\boldsymbol{\eta}$ and $\boldsymbol{\vartheta}$) with $\boldsymbol{g}_h$ by using Lagrange cubic finite elements whose their restriction to a typical element I_h^e is $\boldsymbol{g}_h^e$. This field is interpolated using the Lagrangian shape function as follows

$$\boldsymbol{g}_h^e(s) = \sum_{n=1}^{4} \phi_n^e(s) \boldsymbol{g}_h^{e,n}, \quad \text{such that } \phi_n^e(s) = \phi_n(\frac{s - s_{e-1}}{h}),\ \forall s \in I_h^e, \qquad (7.1)$$

where $(\phi_n(\cdot))_{1 \leq n \leq 4}$ are the usual cubic interpolation functions on a reference element, and $\boldsymbol{g}_h^{e,n}$ represent the nodal value at node n of element e of the field $\boldsymbol{g}_h^e$. The discretizations of the first two integral parts in (4.1) concerning the virtual work of internal forces and external loads are well detailed in [7].

7.1 Discretization of the frictional self-contact energy

We denote by $N_G = \{s_i;\ i = 0, \cdots, N_g\}$ the set of total Gauss quadrature nodes on $[0, l]$. For all $s_i \in N_G$ and I_h^v the slave element that contains the slave node s_i, we denote by I_h^e the corresponding master element that contains the master node $\bar{s}_i$. For the elements of frictional self-contact, we introduce the following vectors of nodal values of $\boldsymbol{r}$ and $\boldsymbol{\theta}$:

$$\boldsymbol{r}^{(v,e)} = \left(\boldsymbol{r}^{v,1}, \boldsymbol{r}^{v,2}, \boldsymbol{r}^{v,3}, \boldsymbol{r}^{v,4}, -\boldsymbol{r}^{e,1}, -\boldsymbol{r}^{e,2}, -\boldsymbol{r}^{e,3}, -\boldsymbol{r}^{e,4}\right)^T,$$
$$\boldsymbol{\theta}^{(v,e)} = \left(\boldsymbol{\theta}^{v,1}, \boldsymbol{\theta}^{v,2}, \boldsymbol{\theta}^{v,3}, \boldsymbol{\theta}^{v,4}, -\boldsymbol{\theta}^{e,1}, -\boldsymbol{\theta}^{e,2}, -\boldsymbol{\theta}^{e,3}, -\boldsymbol{\theta}^{e,4}\right)^T.$$

By substitution of the finite-element approximations defined at the beginning of this section, the discretized form of the contact energy (6.2) writes

$$\mathcal{G}_{\mathrm{c}} = \sum_{v=1}^{N} \mathcal{G}_c^v = -\sum_{v=1}^{N} \int_{I_h^v} \begin{pmatrix} f_N^{\mu_N} \boldsymbol{N}^v + \boldsymbol{f}_{\mathrm{T}}^{\mu_{\mathrm{T}}} \\ \boldsymbol{f}_{\mathrm{R}}^{\mu_{\mathrm{R}}} \end{pmatrix} \cdot \begin{pmatrix} \Sigma_{n=1}^4 \phi_n^v \delta\boldsymbol{r}_h^{v.n} - \Sigma_{n=1}^4 \breve{\phi}_n^e \delta\boldsymbol{r}_h^{e.n} \\ \Sigma_{n=1}^4 \phi_n^v \delta\boldsymbol{\theta}_h^{v.n} - \Sigma_{n=1}^4 \breve{\phi}_n^e \delta\boldsymbol{\theta}_h^{e.n} \end{pmatrix} ds.$$

For what follows, by introducing $\boldsymbol{\Psi}_N^{(v,e)}$, $\boldsymbol{\Psi}_{\mathrm{T}}^{(v,e)}$ and $\boldsymbol{\Psi}_{\mathrm{R}}^{(v,e)}$ the discretizations of the normal, tangential and rotational self-contact forces defined by

$$\boldsymbol{\Psi}_N^{(v,e)} = \begin{bmatrix} \phi_1^v f_{\mathrm{N}.v}^{\mu_{\mathrm{N}}} \boldsymbol{N}^v \\ \phi_2^v f_{\mathrm{N}.v}^{\mu_{\mathrm{N}}} \boldsymbol{N}^v \\ \phi_3^v f_{\mathrm{N}.v}^{\mu_{\mathrm{N}}} \boldsymbol{N}^v \\ \phi_4^v f_{\mathrm{N}.v}^{\mu_{\mathrm{N}}} \boldsymbol{N}^v \\ -\breve{\phi}_1^e f_{\mathrm{N}.v}^{\mu_{\mathrm{N}}} \boldsymbol{N}^v \\ -\breve{\phi}_2^e f_{\mathrm{N}.v}^{\mu_{\mathrm{N}}} \boldsymbol{N}^v \\ -\breve{\phi}_3^e f_{\mathrm{N}.v}^{\mu_{\mathrm{N}}} \boldsymbol{N}^v \\ -\breve{\phi}_4^e f_{\mathrm{N}.v}^{\mu_{\mathrm{N}}} \boldsymbol{N}^v \end{bmatrix}, \ \boldsymbol{\Psi}_{\mathrm{T}}^{(v,e)} = \begin{bmatrix} \phi_1^v \boldsymbol{f}_{\mathrm{T}.v}^{\mu_{\mathrm{T}}} \\ \phi_2^v \boldsymbol{f}_{\mathrm{T}.v}^{\mu_{\mathrm{T}}} \\ \phi_3^v \boldsymbol{f}_{\mathrm{T}.v}^{\mu_{\mathrm{T}}} \\ \phi_4^v \boldsymbol{f}_{\mathrm{T}.v}^{\mu_{\mathrm{T}}} \\ -\breve{\phi}_1^e \boldsymbol{f}_{\mathrm{T}.v}^{\mu_{\mathrm{T}}} \\ -\breve{\phi}_2^e \boldsymbol{f}_{\mathrm{T}.v}^{\mu_{\mathrm{T}}} \\ -\breve{\phi}_3^e \boldsymbol{f}_{\mathrm{T}.v}^{\mu_{\mathrm{T}}} \\ -\breve{\phi}_4^e \boldsymbol{f}_{\mathrm{T}.v}^{\mu_{\mathrm{T}}} \end{bmatrix}, \ \boldsymbol{\Psi}_{\mathrm{R}}^{(v,e)} = \begin{bmatrix} \phi_1^v \boldsymbol{f}_{\mathrm{R}.v}^{\mu_{\mathrm{R}}} \\ \phi_2^v \boldsymbol{f}_{\mathrm{R}.v}^{\mu_{\mathrm{R}}} \\ \phi_3^v \boldsymbol{f}_{\mathrm{R}.v}^{\mu_{\mathrm{R}}} \\ \phi_4^v \boldsymbol{f}_{\mathrm{R}.v}^{\mu_{\mathrm{R}}} \\ -\breve{\phi}_1^e \boldsymbol{f}_{\mathrm{R}.v}^{\mu_{\mathrm{R}}} \\ -\breve{\phi}_2^e \boldsymbol{f}_{\mathrm{R}.v}^{\mu_{\mathrm{R}}} \\ -\breve{\phi}_3^e \boldsymbol{f}_{\mathrm{R}.v}^{\mu_{\mathrm{R}}} \\ -\breve{\phi}_4^e \boldsymbol{f}_{\mathrm{R}.v}^{\mu_{\mathrm{R}}} \end{bmatrix},$$

and by using a Gaussian quadrature rule with three integration points for approximating the integral over I_h^v, we can write

$$\mathcal{G}_{\mathrm{c}} \simeq \sum_{v=1}^{N}\sum_{i=1}^{3} \begin{pmatrix} \boldsymbol{F}_{\mathrm{NT}}^{v,i} \\ \boldsymbol{F}_{\mathrm{R}}^{v,i} \end{pmatrix} \cdot \begin{pmatrix} \delta\boldsymbol{r}^{(v,e_i)} \\ \delta\boldsymbol{\theta}^{(v,e_i)} \end{pmatrix},$$

where $(\boldsymbol{F}_{\mathrm{NT}}^{v,i}, \boldsymbol{F}_{\mathrm{R}}^{v,i})^T = -\omega_i \big(\boldsymbol{\Psi}_{\mathrm{N}}^{(v,e_i)} + \boldsymbol{\Psi}_{\mathrm{T}}^{(v,e_i)}, \boldsymbol{\Psi}_{\mathrm{R}}^{(v,e_i)}\big)^T$ represents the discretized frictional self-contact forces applied to element v, and ω_i are the corresponding Gauss integration weights.

We similarly use the finite-element approximation (7.1) and the Gaussian quadrature rule with three integration points for evaluating the integrals in the expression (6.8) to obtain their discretized form

$$\begin{aligned} \Delta\mathcal{G}_{\mathrm{c}} &= \sum_{v=1}^{N} \Delta\mathcal{G}_{\mathrm{c}}^{v} \\ &\simeq \sum_{v=1}^{N}\sum_{i=1}^{3} \omega_i \left((\Delta\boldsymbol{r}^{(v,e_i)})^T \mathbb{K}_{\mathrm{NT}}^{v,i} \delta\boldsymbol{r}^{(v,e_i)} + \begin{pmatrix} \Delta\boldsymbol{r}^{(v,e_i)} \\ \Delta\boldsymbol{\theta}^{(v,e_i)} \end{pmatrix}^T \begin{pmatrix} \mathbb{K}_{\mathrm{R1}}^{v,i} \\ \mathbb{K}_{\mathrm{R2}}^{v,i} \end{pmatrix} \delta\boldsymbol{\theta}^{(v,e_i)} \right) \end{aligned}$$

where $\mathbb{K}_{\mathrm{NT}}^{v,i}$ and $(\mathbb{K}_{\mathrm{R1}}^{v,i},\ \mathbb{K}_{\mathrm{R2}}^{v,i})$ are the frictional self-contact element stiffness matrices given as follows

$$\mathbb{K}_{\mathrm{NT}}^{v,i} = \frac{H(d_{\boldsymbol{r}}^{(v,e)} + \mu_{\mathrm{N}}\lambda_{\mathrm{N}}^{n,(v,e)})}{\mu_{\mathrm{N}}(2\varepsilon - d_{\boldsymbol{r}}^{(v,e)})} (\boldsymbol{\Sigma}_1^{(v,e_i)})^T \boldsymbol{\Gamma}_{\mathrm{N}}^{(v,e_i)} \boldsymbol{\Sigma}_1^{(v,e_i)} + (\boldsymbol{\Sigma}_1^{(v,e_i)})^T \boldsymbol{\Gamma}_{\mathrm{T}}^{(v,e_i)} \boldsymbol{\Sigma}_1^{(v,e_i)},$$

$$(\mathbb{K}_{\mathrm{R1}}^{v,i},\ \mathbb{K}_{\mathrm{R2}}^{v,i}) = \left((\boldsymbol{\Sigma}_1^{(v,e_i)})^T \boldsymbol{\Gamma}_{\mathrm{R1}}^{(v,e_i)} \boldsymbol{\Sigma}_1^{(v,e_i)},\ \ (\boldsymbol{\Sigma}_1^{(v,e_i)})^T \boldsymbol{\Gamma}_{\mathrm{R2}}^{(v,e_i)} \boldsymbol{\Sigma}_2^{(v,e_i)} \right)$$

where

$$\boldsymbol{\Gamma}_{\mathrm{N}}^{(v,e)} = \begin{bmatrix} \boldsymbol{\Gamma}_{\mathrm{N},11}^{(v,e)} & \boldsymbol{\Gamma}_{\mathrm{N},12}^{(v,e)} \\ \boldsymbol{\Gamma}_{\mathrm{N},21}^{(v,e)} & \boldsymbol{\Gamma}_{\mathrm{N},22}^{(v,e)} \end{bmatrix},\ \boldsymbol{\Gamma}_{\mathrm{T}}^{(v,e)} = \begin{bmatrix} \boldsymbol{\Gamma}_{\mathrm{T}.11}^{(v,e)} & \boldsymbol{\Gamma}_{\mathrm{T}.12}^{(v,e)} \\ \boldsymbol{\Gamma}_{\mathrm{T}.21}^{(v,e)} & \boldsymbol{\Gamma}_{\mathrm{T}.22}^{(v,e)} \end{bmatrix},\ \boldsymbol{\Gamma}_{\mathrm{R1}}^{(v,e)} = \begin{bmatrix} \boldsymbol{\Gamma}_{\mathrm{R1}.11}^{(v,e)} & \boldsymbol{\Gamma}_{\mathrm{R1}.12}^{(v,e)} \\ \boldsymbol{\Gamma}_{\mathrm{R1}.21}^{(v,e)} & \boldsymbol{\Gamma}_{\mathrm{R1}.22}^{(v,e)} \end{bmatrix},$$

$$\boldsymbol{\Gamma}_{\mathrm{R2}}^{(v,e)} = \begin{bmatrix} -\frac{\Xi_{\mathrm{R}}^{(v,e)}}{2} & \boldsymbol{0} \\ \frac{(\bar{s}-\bar{s}_0)\Xi_{\mathrm{R}}^{(v,e)}}{2} & \boldsymbol{0} \end{bmatrix},\ \boldsymbol{\Sigma}_1^{(v,e)} = \begin{bmatrix} \boldsymbol{\Phi}^v & -\breve{\boldsymbol{\Phi}}^e \\ \boldsymbol{0} & \breve{\boldsymbol{\Phi}}^{e\prime} \end{bmatrix},\ \boldsymbol{\Sigma}_2^{(v,e)} = \begin{bmatrix} \boldsymbol{\Phi}^v & -\breve{\boldsymbol{\Phi}}^e \\ \boldsymbol{0} & \boldsymbol{0} \end{bmatrix},$$

$$\boldsymbol{\Phi}^e = \left[\phi_1^e \boldsymbol{I}\ \phi_2^e \boldsymbol{I}\ \phi_3^e \boldsymbol{I}\ \phi_4^e \boldsymbol{I}\right],$$

with

$$\boldsymbol{\Gamma}_{\mathrm{N}.11}^{(v,e)} = \frac{d_{\boldsymbol{r}}^{(v,e)}}{\|\breve{\boldsymbol{r}}^{e\prime}\|^2 - \breve{\boldsymbol{r}}^{e\prime\prime} \cdot (\boldsymbol{r}^v - \breve{\boldsymbol{r}}^e)} \breve{\boldsymbol{r}}^{e\prime} \otimes \breve{\boldsymbol{r}}^{e\prime} + 2\varepsilon \boldsymbol{N}^v \otimes \boldsymbol{N}^v - d_{\boldsymbol{r}}^v \boldsymbol{I},$$

$$\boldsymbol{\Gamma}_{\mathrm{N}.12}^{(v,e)} = \frac{d_{\boldsymbol{r}}^{(v,e)}}{\|\breve{\boldsymbol{r}}^{e\prime}\|^2 - \breve{\boldsymbol{r}}^{e\prime\prime} \cdot (\boldsymbol{r}^v - \breve{\boldsymbol{r}}^e)} \breve{\boldsymbol{r}}^{e\prime} \otimes (\boldsymbol{r}^v - \breve{\boldsymbol{r}}^e),$$

$$\boldsymbol{\Gamma}_{\mathrm{N}.21}^{(v,e)} = \frac{d_{\boldsymbol{r}}^{(v,e)}}{\|\breve{\boldsymbol{r}}^{e\prime}\|^2 - \breve{\boldsymbol{r}}^{e\prime\prime} \cdot (\boldsymbol{r}^v - \breve{\boldsymbol{r}}^e)} (\boldsymbol{r}^v - \breve{\boldsymbol{r}}^e) \otimes \breve{\boldsymbol{r}}^{e\prime},$$

$$\boldsymbol{\Gamma}^{(v,e)}_{\mathrm{N}.22} = \frac{d^{(v,e)}_{\boldsymbol{r}}}{\|\breve{\boldsymbol{r}}^{e\prime}\|^2 - \breve{\boldsymbol{r}}^{e\prime\prime}\cdot(\boldsymbol{r}^v - \breve{\boldsymbol{r}}^e)}(\boldsymbol{r}^v - \breve{\boldsymbol{r}}^e)\otimes(\boldsymbol{r}^v - \breve{\boldsymbol{r}}^e),$$

$$\boldsymbol{\Gamma}^{(v,e)}_{\mathrm{T}.11} = \frac{1}{\|\breve{\boldsymbol{r}}^{e\prime}\|^2 - \breve{\boldsymbol{r}}^{e\prime\prime}\cdot(\boldsymbol{r}^v - \breve{\boldsymbol{r}}^e)}\Xi^{(v,e)}_{\mathrm{T}}\breve{\boldsymbol{r}}^{e\prime}\otimes\breve{\boldsymbol{r}}^{e\prime} + \frac{\Xi^{(v,e)}_{\mathrm{T}}}{4\varepsilon - d^v_{\boldsymbol{r}}}\big(2\varepsilon\boldsymbol{N}^v\otimes\boldsymbol{N}^v - d^v_{\boldsymbol{r}}\boldsymbol{I}\big),$$

$$\boldsymbol{\Gamma}^{(v,e)}_{\mathrm{T}.12} = \frac{1}{\|\breve{\boldsymbol{r}}^{e\prime}\|^2 - \breve{\boldsymbol{r}}^{e\prime\prime}\cdot(\boldsymbol{r}^v - \breve{\boldsymbol{r}}^e)}\breve{\boldsymbol{r}}^{e\prime}\otimes\boldsymbol{f}^{\mu_{\mathrm{T}}}_{\mathrm{T}.v},$$

$$\boldsymbol{\Gamma}^{(v,e)}_{\mathrm{T}.21} = \frac{1}{\|\breve{\boldsymbol{r}}^{e\prime}\|^2 - \breve{\boldsymbol{r}}^{e\prime\prime}\cdot(\boldsymbol{r}^v - \breve{\boldsymbol{r}}^e)}\Xi^{(v,e)}_{\mathrm{T}}(\boldsymbol{r}^v - \breve{\boldsymbol{r}}^e)\otimes\breve{\boldsymbol{r}}^{e\prime},$$

$$\boldsymbol{\Gamma}^{(v,e)}_{\mathrm{T}.22} = \frac{1}{\|\breve{\boldsymbol{r}}^{e\prime}\|^2 - \breve{\boldsymbol{r}}^{e\prime\prime}\cdot(\boldsymbol{r}^v - \breve{\boldsymbol{r}}^e)}(\boldsymbol{r}^v - \breve{\boldsymbol{r}}^e)\otimes\boldsymbol{f}^{\mu_{\mathrm{T}}}_{\mathrm{T}.v},$$

$$\boldsymbol{\Gamma}^{(v,e)}_{\mathrm{R}1.11} = \frac{1}{\|\breve{\boldsymbol{r}}^{e\prime}\|^2 - \breve{\boldsymbol{r}}^{e\prime\prime}\cdot(\boldsymbol{r}^v - \breve{\boldsymbol{r}}^e)}\Xi^{(v,e)}_{\mathrm{R}}\breve{\boldsymbol{r}}^{e\prime}\otimes(\breve{\boldsymbol{\theta}}^{e\prime} + \frac{\bar{s}-\bar{s}_0}{2}\breve{\boldsymbol{\theta}}^{e\prime\prime}),$$

$$\boldsymbol{\Gamma}^{(v,e)}_{\mathrm{R}1.12} = \frac{1}{\|\breve{\boldsymbol{r}}^{e\prime}\|^2 - \breve{\boldsymbol{r}}^{e\prime\prime}\cdot(\boldsymbol{r}^v - \breve{\boldsymbol{r}}^{e\prime})}\breve{\boldsymbol{r}}^{e\prime}\otimes\boldsymbol{f}^{\mu_{\mathrm{R}}}_{\mathrm{R}.v},$$

$$\boldsymbol{\Gamma}^{(v,e)}_{\mathrm{R}1.21} = \frac{1}{\|\breve{\boldsymbol{r}}^{e\prime}\|^2 - \breve{\boldsymbol{r}}^{e\prime\prime}\cdot(\boldsymbol{r}^v - \breve{\boldsymbol{r}}^e)}\Xi^{(v,e)}_{\mathrm{R}}(\boldsymbol{r}^v - \breve{\boldsymbol{r}}^e)\otimes(\breve{\boldsymbol{\theta}}^{e\prime} + \frac{\bar{s}-\bar{s}_0}{2}\breve{\boldsymbol{\theta}}^{e\prime\prime}),$$

$$\boldsymbol{\Gamma}^{(v,e)}_{\mathrm{R}1.22} = \frac{1}{\|\breve{\boldsymbol{r}}^{e\prime}\|^2 - \breve{\boldsymbol{r}}^{e\prime\prime}\cdot(\boldsymbol{r}^v - \breve{\boldsymbol{r}}^e)}(\boldsymbol{r}^v - \breve{\boldsymbol{r}}^e)\otimes\boldsymbol{f}^{\mu_{\mathrm{T}}}_{\mathrm{R}.v},$$

and

$$\Xi^{(v,e)}_{\mathrm{T}} = \frac{F_{\mathrm{T}}\big(\boldsymbol{g}^{(v,e)}_{\boldsymbol{r}} + \mu_{\mathrm{T}}\boldsymbol{\lambda}^{n,(v,e)}_{\mathrm{T}}\big)(4\varepsilon - d^{(v,e)}_{\boldsymbol{r}})}{\mu_{\mathrm{T}}\Delta t(2\varepsilon - d^{(v,e)}_{\boldsymbol{r}})}, \quad \Xi^{(v,e)}_{\mathrm{R}} = \frac{2F_{\mathrm{R}}\big(\boldsymbol{g}^{(v,e)}_{\boldsymbol{R}} + \mu_{\mathrm{R}}\boldsymbol{\lambda}^{n,(v,e)}_{\mathrm{R}}\big)}{\mu_{\mathrm{R}}\Delta t}.$$

It should be noted that the stiffness matrices $\mathbb{K}^{v,i}_{\mathrm{NT}}$ and $\mathbb{K}^{v,i}_{\mathrm{R}1}$ are symmetric, whereas the stiffness matrix $\mathbb{K}^{v,i}_{\mathrm{R}2}$ is nonsymmetric. In the stability analysis, which is based on resolving an eigenvalue problem, it is highly desirable to have a method to symmetrize the stiffness matrix $\mathbb{K}^{v,i}_{\mathrm{R}2}$ as well as the geometric part of the tangential element stiffness matrix given by Chamekh et al. [7]. For more details on the symmetrization technique see [13, 26].

8 Conclusions

One of the most important points in these types of problems is the existence result for the theoretical formulation. Unfortunately, the self-friction problem in elastic rods is strongly nonlinear due to the coupling between the displacement and rotation. As in the tangential self-friction case, the existence and uniqueness of the solution remain a major challenge in the rotational self-friction case. We have used the augmented Lagrangian method to present a weak nonlinear variational formulation approach and have given an existence theorem for the penalized problem. Newton-Raphson method is proposed to relax the problem of this nonlinearity. In addition, linearization and discretization by finite-elements are well developed, which perhaps facilitates the numerical implementation in future research.

Data availability statement

Data sharing not applicable to this article as no datasets were generated or analysed during the current study.

Acknowledgements The authors are pleased to be able to thank Prof. Yves Renard for his several fruitful discussions during this paper, and they are also very grateful for the helpful and constructive comments of the anonymous reviewers.

Conflict of interest

The authors declare that they have no conflict of interest regarding the publication of this article.

References

1. Antman. S. S.: *Nonlinear Problems of Elasticity*, 2nd ed, Applied Mathematical Sciences, Springer Verlag, New York, (2004).
2. Bozorgmehri. B., Yu. X., Matikainen. M. K., Harish. A. B., Mikkola. A.: *A study of contact methods in the application of large deformation dynamics in self-contact beam.* Nonlinear Dyn **103**, 581–616 (2021)
3. Bourgat. J. F., Le Tallec. P., Mani. S.: *Modlisation et calcul des grands dplacements de tuyaux lastiques en flexion-torsion.* J. Mcanique Thor. Appl, **7**(4), 379408 (1988)
4. Béal. P., Touzani. R.: *Analysis of contact of elastic rods subject to large displacements.* Applied Mathematics Letters **16**, 619–625 (2003)
5. Cosserat. E., Cosserat. F.: *Théorie des Corps Déformables*, Hermann, Paris (1909)
6. Chouly. F., Hild. P., Lleras. V., Renard. Y.: *Nitsche method for contact with Coulomb friction: existence results for the static and dynamic finite element formulations.* hal-02938032, (2020)
7. Chamekh. M., Mani-Aouadi. S., Moakher. M.: *Modeling and numerical treatment of elastic rods with frictionless self-contact.* Comput. Methods Appl. Mech. Engrg, **198**(47/48), 3751–3764 (2009)
8. Chamekh. M., Latrach. M. A., Renard. Y.: *Frictional self-contact problem of elastic rods.* Journal of King Saud University-Science. Elsevier BV. **32**, 828–835 (2020)
9. Demanget. N., Avril. S., Badel. P., Orgéas. L., Geindreau. C., Albertini. J-N., Favre; J-P.: *Computational comparison of the bending behavior of aortic stentgrafts.* J. Mech. Behav. Biomed. Mater, **5**, 272–282 (2012)
10. Demanget. N., Duprey. A., Badel. P., Orgéas. L., Avril. S., Geindreau. C., Albertini. J-N., Favre; J-P.: *Finite element analysis of the mechanical performances of marketed aortic stent-grafts.* J. Endovasc. Ther. **20**, 523–535 (2013)
11. Goicoechea. H. E., Buezas. F. S., Rosales. M. B.: *A non-linear Cosserat rod model for drill-string dynamics in arbitrary borehole geometries with contact and friction.* International Journal of Mechanical Sciences 157–158, 98-110, (2019)
12. Goyal. S., Perkins. N. C., Lee. C. L.: *Nonlinear dynamics and loop formation in Kirchhoff rods with implications to the mechanics of DNA and cables.* J. Comput. Phys, **209**, 371–389 (2005)
13. Ibrahimbegović. A.: *On the choice of finite rotation parameters.* Comput. Methods Appl. Mech. Engrg, **149**(1/4), 49–71 (1997)
14. Kerrien. E., Yureidini. A., Dequidt. J., Duriez. C., Anxionnat. R., Cotin. S.: *Blood vessel modeling for interactive simulation of interventional neuroradiology procedures.* Medical Image Analysis **35**, 685–698 (2017)
15. Kikuchi. N., Oden. J. T.: *Contact Problems in Elasticity: A Study of Variational Inequalities and Finite Element Methods*, SIAM, Philadelphia (1988)

16. Lu, C., Perkins. N.: *Complex spatial equilibria of U-joint supported cables under torque, trust and self-weight.* International Journal of Nonlinear Mechanics, **30**, 271–285, (1995)
17. Latrach. M. A.: *Problème de l'auto-contact avec frottement dans une tige élastique et solutions analytiques approximatives pour des problèmes d'obstacles.* Mathématiques [math]. Université de Tunis El Manar- École Nationale d'Ingnieurs de Tunis, 2020. Français. tel-03091354
18. Moakher. M., Maddocks. J. H.: *A double-strand elastic rod theory.* Archive for Rational Mechanics and Analysis, **177**, 53–91, (2005)
19. Mlika. R., Renard. Y., Chouly. F.: *An unbiased Nitsche's formulation of large deformation frictional contact and self-contact.* Computer Methods in Applied Mechanics and Engineering, Elsevier, **325**, 265–288 (2017)
20. Perrin. D., Badel. P., Orgéas. L., Geindreau. C., Dumenil. A., Albertini. J-N., Avril. S.: *Patient-specific numerical simulation of stent-graft deployment: Validation on three clinical cases.* Journal of Biomechanics **48**(10), 1868–1875 (2015)
21. Peng. L., Feng. Z. Q., Joli. P., Liu. J. H., Zhou. Y. J.: *Automatic contact detection between rope fibers.* Computers & Structures, **218**, 82-93, ISSN 0045-7949 (2019)
22. Reissner. E.: *On finite deformations of space curved beams.* Journal of Applied Mathematical Physics, **32**, 734–744 (1981)
23. Renard. Y.: *A uniqueness criterion for the Signorini problem with Coulomb friction.* SIAM journal on mathematical analysis **38**(2), 452–467, (2006)
24. Stump. D. M.: *The hockling of cables: A problem in shearable and extensible rods.* International Journal of Solids and Structures, **37**, 515–533, (2000)
25. Simo. J. C. , Vu-Quoc. L.: *On the dynamics in space of rods undergoing large motions – A geometrically exact approach.* Comput. Methods Appl. Mech. Engrg, **66**(2), 125–161 (1988)
26. Simo. J. C.: *The (symmetric) hessian for geometrically nonlinear models in solid mechanics: Intrinsic definition and geometric interpretation.* Comput. Methods Appl. Mech. Engrg, **96**, 189–200 (1992)
27. White. D. J., Randolph. M. F.: *Seabed characterisation and models for pipeline-soil interaction.* in: Proceedings of the International Offshore and Polar Engineering Conference, International Society of Offshore and Polar Engineers, pp. 758–769 (2007)
28. Yabuta. T.: *Submarine cable kink analysis.* Bulletin of the Japanese Society of Mechanical Engineers, **27**(584), 1821–1828, (1984)